

Coordination of Generation Scheduling with PEVs Charging in Industrial Microgrids

S. Y. Derakhshandeh, *Student Member, IEEE*, Amir S. Masoum, *Member, IEEE*, Sara Deilami, *Student Member, IEEE*, Mohammad A. S. Masoum, *Senior Member, IEEE*, and M. E. Hamedani Golshan

Abstract—Conventional industrial microgrids (IMGs) consist of factories with distributed energy resources (DERs) and electric loads that rely on combined heat and power (CHP) systems while the developing IMGs are expected to also include renewable DERs and plug-in electric vehicles (PEVs) with different vehicle ratings and charging characteristics. This paper presents an electricity and heat generation scheduling method coordinated with PEV charging in an IMG considering photovoltaic (PV) generation systems coupled with PV storages. The proposed method is based on dynamic optimal power flow (DOPF) over a 24-hour period and includes security-constrained optimal power flow (SCOPF), IMG's factories constraints, PV storage constraints and PEVs dynamic charging constraints. It will utilize the generators waste heat to fulfill thermal requirements while considering the status of renewable DERs to decrease the overall cost of IMGs. To demonstrate the effectiveness of the proposed method, detailed simulation results are presented and analyzed for an 18-bus IMG consisting of 12 factories and 6 types of PEVs without/with PV generation systems operating in grid-connected and stand-alone modes. The main contribution is including PEVs with dynamic constraints that have changed the nature of scheduling formulation from a simple hourly OPF to a dynamic OPF.

Index Terms—Combined heat and power (CHP), dynamic optimal power flow, industrial microgrid, photovoltaic (PV), plug-in electric vehicle (PEV).

NOMENCLATURE

h	Hour index.
i, j	Bus indices.
k	Vehicle index.
l	Thermal group index.

$b_{i,h}$	Heat generation via the boiler of the factory connected to bus i at hour h (kW).
b_i^{max}	Maximum output of the boiler of the factory connected to bus i (kW).
$Cost$	Cost imposed on IMG (\$).
$Cost_{i,h}^b$	Cost of generating heat via boiler at the factory connected to bus i at hour h (\$).
$Cost_{i,h}^{CHP}$	Cost of generating electricity with CHP system at the factory connected to bus i at hour h (\$).
$Cost_{i,h}^{PV}$	Cost of generating electricity with PV generation system at factory connected to bus i at hour h (\$).
D_l^{th}	Thermal power required by group l at hour h (kW).
ep_h	Electricity price at hour h in the upstream network (\$/kWh).
$E_{i,h}^S$	Energy stored in PV storage of the factory connected to bus i at hour h (kWh).
$E_i^{S,max}$	Maximum energy capacity of PV storage at factory connected to bus i (kWh).
$E_i^{S,min}$	Minimum state of charge of PV storage at factory connected to bus i (kWh).
$E_{k,h}^V$	Energy stored in vehicle k at the end of hour h (kWh).
$E_k^{V,max}$	Battery energy capacity of vehicle k (kWh).
G_{ij}, B_{ij}	Real and imaginary elements in the i th row and j th column of node admittance matrix (mho).
gp	Gas price (\$/kWh).
$grid_h^{buy}$	Purchased electricity by the IMG from the upstream network at hour h (kW).
$grid_h^{sell}$	Electricity sold to upstream network by the IMG at hour h (kW).
$h_{po,k}$	Preferred plug-out time of PEV k .
HR_i^{CHP}	Heat rate of CHP system of the factory connected to bus i (kJ/kWh).
N	Number of buses.

Manuscript received October 06, 2012; revised February 04, 2013; accepted March 26, 2013. Paper no. TPWRS-01132-2012.

S. Y. Derakhshandeh and M. E. Hamedani Golshan are with the Department of Electrical and Computer Engineering, Isfahan University of Technology, Isfahan, Iran (e-mail: y_derakhshandeh@ec.iut.ac.ir; hgolshan@cc.iut.ac.ir).

A. S. Masoum is with Transmission Maintenance Delivery, Western Power, WA, Australia (e-mail: a_masoum@iee.org).

S. Deilami and M. A. S. Masoum are with the Department of Electrical and Computer Engineering, Curtin University, WA, Australia (e-mail: s.deilami@postgrad.curtin.edu.au; m.masoum@curtin.edu.au).

Color versions of one or more of the figures in this paper are available online at <http://ieeexplore.ieee.org>.

Digital Object Identifier 10.1109/TPWRS.2013.2257184

OM_i^{CHP}	Operation and maintenance variable cost of CHP system in the factory connected to bus i (\$/kWh).	T	Number of intervals (hour).
OM_i^{PV}	Operation and maintenance variable cost of PV panels in the factory connected to bus i (\$/kWh).	th_l	l th group of factories that can exchange heat between themselves.
<i>Overall Cost</i>	Overall cost during the schedule period (\$).	$V_{i,h}$	Voltage of bus i at hour h (V).
$P_{i,h}^{CHP}$	Active power generation via CHP system of the factory connected to bus i at hour h (kW).	V_i^{min}, V_i^{max}	Minimum and maximum limits of voltage at bus i (V).
$P_{i,h}^D$	Total active load power at bus i at hour h (kW).	α_i^{CHP}	Waste heat factor of the CHP system of the factory connected to bus i .
$P_{i,h}^F$	Active power of the factory connected to bus i at hour h (kW).	$\theta_{i,j,h}$	Phase angle difference between nodes i and j at hour h (radian).
$P_{i,h}^G$	Total active power generation at bus i at hour h (kW).	η_i^b	Efficiency of boiler of factory connected to bus i .
$P_{ij,h}$	Power between buses i and j at hour h (kW).	η_i^{CHP}	Electric efficiency of CHP system of the factory connected to bus i .
P_{ij}^{max}	Maximum limit of power flow between buses i and j (kW).	$\eta_i^{S.ch}$	Charging efficiency of PV storage at the factory connected to bus i .
P_i^{min}, P_i^{max}	Minimum and maximum active power of the CHP system of the factory connected to bus i (kW).	$\eta_i^{S.Dch}$	Discharging efficiency of PV storage at the factory connected to bus i .
$P_{i,h}^{PV}$	Predicted PV generation level of the factory connected to bus i at hour h (kW).	η_k^V	Battery charging efficiency of electric vehicle k .
$P_{i,h}^{S.ch}$	Power charge of PV storage at factory connected to bus i at hour h (kW).	Δh	Optimization time interval (hour).
$P_i^{S.ch,max}$	Maximum power charge of PV storage at the factory connected to bus i (kW).		
$P_{i,h}^{S.Dch}$	Power discharge of PV storage at the factory connected to bus i at hour h (kW).		
$P_i^{S.Dch,max}$	Maximum power discharge of PV storage at the factory connected to bus i (kW).		
$P_{i,k,h}^{V.ch}$	Power charge of vehicle k located at the factory connected to bus i at hour h (kW).		
$P_k^{V.ch,max}$	Maximum power charge of vehicle k (kW).		
$Q_{i,h}^{CHP}$	Reactive power generation via CHP system of the factory connected to bus i at hour h (kVAr).		
$Q_{i,h}^D$	Total reactive load power at bus i at hour h (kVAr).		
$Q_{i,h}^F$	Reactive power of the factory connected to bus i at hour h (kVAr).		
$Q_{i,h}^G$	Total reactive power generation at bus i at hour h (kVAr).		
Q_i^{min}, Q_i^{max}	Minimum and maximum reactive power of the CHP system of the factory connected to bus i (kVAr).		
<i>Revenue</i>	Revenue of IMG (\$).		
<i>SC</i>	Sell coefficient.		

I. INTRODUCTION

INDUSTRIAL microgrids (IMGs) rely on combined heat and power (CHP) systems to facilitate energy-efficient power generation by capturing the waste heat. These systems maintain the heat acquired from power generation and utilize it for domestic and industrial heating purposes [1]. Heat produced at moderate temperatures (100–180°C) can also be used in absorption chillers for cooling [1]. Among various types of CHP systems, gas turbine, natural gas engine and micro turbines have major roles in IMGs and industrial parks[2], [3]. Unlike other technologies, they are dispatchable, require lower investment cost and can continuously generate energy for hundreds of hours [4]. Moreover, they have appealing operational flexibility such as fast start up time, fast shut down time and high ramp rate [5]–[8].

Generation scheduling and optimal power flow (OPF) has been thoroughly investigated in the power systems [9]–[11] and microgrids (MGs) [12]–[18]. However, this topic has received limited attention [19], [20] in the developing IMGs due to special requirements such as time and energy related charging constraints of plug-in electric vehicles (PEVs). Generation scheduling and OPF in MGs are easier than the conventional power systems since: 1) there is rarely a congestion problem as loads are mostly located near the generators, 2) it is possible to use generators (DERs) with fewer constraints due to their operational flexibility, and 3) most generators are designated to support their own local electric loads with high priorities.

Reference [12] presents a multiagent system for generation scheduling of microgrids involving two stages: day-ahead and real-time scheduling. The day-ahead scheduling determines hourly power settings of DERs from a day-ahead energy market

without considering network constraints and preparation of heat. The real-time scheduling updates the power settings of the DERs by considering the results of the first stage. The main focus of [13] is to prepare an economic emission load dispatch in a CHP-based MG on the basis of multi-objective optimization compromising between fuel cost and emission without considering selling and purchasing electricity to/from upstream network and PEVs charging. In [14], a central and hierarchical control structure with two market policies is proposed for the operation of MGs. The first policy aims to minimize the cost of energy for the end-users without selling energy to the grid, while the second policy tries to maximize the revenues of the aggregator, by exchanging power with the grid. References [15] and [16] present an OPF method for MGs without considering preparation of heat and exchanging electricity with upstream network. Also [17] presents an optimization procedure for a medium-voltage islanded microgrid without considering line capacity constraints and heat preparation.

With the growing popularity PEVs as more efficient low emission alternatives to the conventional fuel-based vehicles [21], it is expected that their application in IMGs will also increase in the near future. References [22]–[24] have studied the impacts of PEVs and plug-in hybrid electric vehicles (PHEVs) on the operation of power systems while [25]–[27] have considered their influences on distribution networks. In [25], a real-time smart load management control strategy is proposed for the coordination of PEV charging based on online minimization of total cost of generating energy plus the associated grid energy losses in a residential distribution system. Reference [26] describes the basic functions of an electric vehicle charging service provider and presents a method for planning PEV charging that includes grid constraints. Also, [27] has proposed an approach to address the resource management in a smart grid where distributed generations (DGs), PEVs and demand response are managed according to vehicle-to-grid (V2G) users' profiles and requirements. Reference [18] represents an optimal MG operation method with several PEV charge stations which considers network and PEV constraints.

It is expected that the developing IMGs will also incorporate photovoltaic (PV) generation systems to decrease the overall cost. Reference [28] states that PV generation as a sustainable energy recourse should provide up to 12% of electricity demand by 2020, 20% in 2030 and 30% in 2050. Consequently, in industrial sections where the peak of electricity demand usually occurs during the daytime, the application of PV generation systems can have an important role on the IMG operation within the next few years. While some research works have been recently initiated to investigate the generation scheduling problem in power systems and MGs in the presence of PEVs [18], [22]–[27], no major research has been reported on OPF of IMGs with PEV charging activities that will require considering time and energy related dynamic constraints.

The main contribution of this paper is to propose a dynamic OPF (DOPF) formulation for IMGs that will include both IMG security and factories constraints while considering PEV time and energy related charging constraints. In addition, the effect of PV generation systems coupled with PV storages on generation scheduling will also be considered. The proposed method will

be implemented in an IMG consisting of 12 factories with CHP systems, PV generation systems coupled with PV storages and 6 types of PEVs operating in grid-connected and stand-alone modes.

II. INDUSTRIAL MICROGRIDS WITH PEVS AND PV GENERATION SYSTEMS COUPLED WITH PV STORAGES

A. Industrial Microgrids (IMGs)

IMGs are typically formed by the corporation of a few factories with DERs. In this paper, DERs are assumed to be CHP (e.g., gas turbines, natural gas engines and micro turbines) and PV generation systems. Each factory is assumed to have electric loads and some factories may need heat for their production processes that can be obtained from CHP systems or from the boilers. IMGs can be connected or disconnected from the upstream network. In the stand-alone mode, IMGs must generate their own required energy to feed the electric loads through the cooperation of all DG units. In the grid-connected mode, IMGs are permitted to purchase some of their electric needs from the upstream network or even sell electricity to upstream network in some hours of the day. On the other hand, due to the existing distances between factories, only the ones in the vicinity of each other can cooperate to procure the thermal needs. Of course, some factories may not have thermal requirements.

B. Introduction of PEVs in IMGs

Environmental impacts of the petroleum-based transportation along with the increasing oil prices have led to development of electric transportation infrastructures. PEVs are highly efficient and compared with the conventional vehicles have less operating costs and lower carbon emissions. According to [29], utilization of PEVs in residential, commercial and industrial networks are expected to become every popular in the near future. IMGs and industrial parks usually have heavy and large vehicles such as picker trucks, lift trucks, bucket trucks and delivery trucks. The replacement of these heavy vehicles with PEVs in IMGs needs to be carefully investigated as it may have significant impacts on the management and operation of the electrical networks.

C. PV Generation Systems in IMGs

PV systems are being accepted as suitable alternatives to the conventional energy resources due to environmental concerns and transmission congestion management issues. PV power currently represents a low percentage of the global electricity production. However, its applications in industrial networks are expected to grow rapidly since the peaks of most industrial loads usually coincide with the maximum output of the PV modules. IMGs can utilize the energy generated by PV plants to minimize the cost associated with the operation of thermal units.

PV systems are often coupled with PV storages such as batteries (Fig. 1). This configuration allows IMGs to store the excess generated energy in PV storage elements during off-peak hours and return it back to the system at appropriate times. This arrangement can moderately mitigate the stochastic nature of

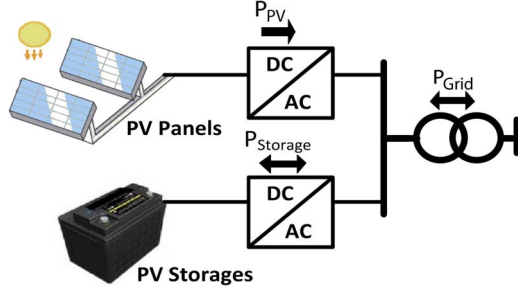


Fig. 1. Simplified configuration of PV generation system coupled with PV storage [30].

the PV production in real time [30] and also increase the profit by selling the stored energy during peak hours [31].

III. FORMULATION OF ELECTRICITY AND HEAT GENERATION SCHEDULING IN IMGs

The proposed formulation of electricity and heat scheduling in an IMG is a DOPF problem over a 24-hour period. This formulation minimizes the overall cost of providing electricity and heat in an IMG subject to electricity and heat requirements as well as network security constraints. The presence of PEVs with high power ratings, time and energy related constraints in IMG will make the generation scheduling more complicated than the conventional OPF. Furthermore, installation of PV generation systems coupled with PV storages may have significant impacts on the scheduling of IMG. Therefore, a new formulation that may be utilized by the MG controller (MGC) will be defined for generation scheduling that will include IMG network security constraints, factories constraints and PV storage constraints, as well as PEVs dynamic constraints while utilizing generators waste heat to fulfill thermal requirements.

A. Objective Function

The objective function of the proposed DOPF is to minimize the overall cost during the schedule period (in this paper, the schedule period is selected to be 24 hours):

$$\text{Minimize } \{ \text{Overall Cost} = \text{Cost} - \text{Revenue} \}. \quad (1)$$

The cost imposed on IMG is divided into four parts corresponding to the costs of electricity production by CHP systems [32], heat production by the boilers [33], the total operation cost of PV generation systems [34], [35] and electricity purchased from upstream network:

$$\begin{aligned} \text{Cost} = & \sum_{i=1}^N \sum_{h=1}^T \text{Cost}_{i,h}^{CHP} + \sum_{i=1}^N \sum_{h=1}^T \text{Cost}_{i,h}^b \\ & + \sum_{i=1}^N \sum_{h=1}^T \text{Cost}_{i,h}^{PV} + \sum_{h=1}^T ep_h * grid_h^{buy} \end{aligned} \quad (2)$$

where

$$\text{Cost}_{i,h}^{CHP} = \left(\frac{P_{i,h}^{CHP}}{\eta_i^{CHP}} * gp \right) + P_{i,h}^{CHP} * OM_i^{CHP} \quad (3)$$

$$\eta_i^{CHP} = \frac{1}{\frac{HR_i^{CHP}}{3600}} \quad (4)$$

$$\text{Cost}_{i,h}^b = \frac{b_{i,h}}{\eta_i^b} * gp \quad (5)$$

$$\text{Cost}_{i,h}^{PV} = P_{i,h}^{PV} * OM_i^{PV}. \quad (6)$$

In (1), the revenue is attained by selling electricity to the upstream network during some hours of the day and expressed as

$$\text{Revenue} = \sum_{h=1}^T SC * ep_h * grid_h^{sell}. \quad (7)$$

B. Decision Variables

The objective function is minimized by determining the control variables. In this paper, the decision variables are active and reactive power generation via CHP systems ($P_{i,h}^{CHP}$, $Q_{i,h}^{CHP}$), heat generation via boilers ($b_{i,h}$), purchased and sold electricity from/to the upstream network ($grid_h^{buy}$, $grid_h^{sell}$), power charge and discharge of PV storages ($P_{i,h}^{S,Ch}$, $P_{i,h}^{S,Dch}$) and power charge of vehicles ($P_{i,k,h}^{V,Ch}$).

C. Problem Constraints

The optimization problem is solved based on the following equality and inequality constraints:

- Power flow equations

$$V_{i,h} \sum_{j=1}^N V_{j,h} (G_{ij} \cos \theta_{ij,h} + B_{ij} \sin \theta_{ij,h}) - P_{i,h}^G + P_{i,h}^D = 0 \quad (8)$$

$$V_{i,h} \sum_{j=1}^N V_{j,h} (G_{ij} \sin \theta_{ij,h} - B_{ij} \cos \theta_{ij,h}) - Q_{i,h}^G + Q_{i,h}^D = 0 \quad (9)$$

where

$$P_{i,h}^G = P_{i,h}^{CHP} + P_{i,h}^{PV} + P_{i,h}^{S,Dch} \quad (10)$$

$$P_{i,h}^D = P_{i,h}^F + P_{i,h}^{S,Ch} + \sum_{k \in i} P_{i,k,h}^{V,Ch} \quad (11)$$

$$Q_{i,h}^G = Q_{i,h}^{CHP} \quad (12)$$

$$Q_{i,h}^D = Q_{i,h}^F. \quad (13)$$

The predicted supplied PV power $P_{i,h}^{PV}$ is determined based on PV specifications (characteristics) and the state of charge of batteries (PV storages). Equations (10) and (11) state that the total generated active power at bus i at each hour is resulted from CHP and PV generation systems and PV storage discharge power while the total active load power at each bus is the summation of the factory demand power, PV storage charge power and electric vehicle charging power. This paper assumes that PV generation systems and PV storages will not participate in reactive power generation and consumption.

- Heat requirement for each thermal group[36]

$$\sum_{i \in th_i} (\alpha_i^{CHP} * P_{i,h}^{CHP} + b_{i,h}) \geq D_i^{th}. \quad (14)$$

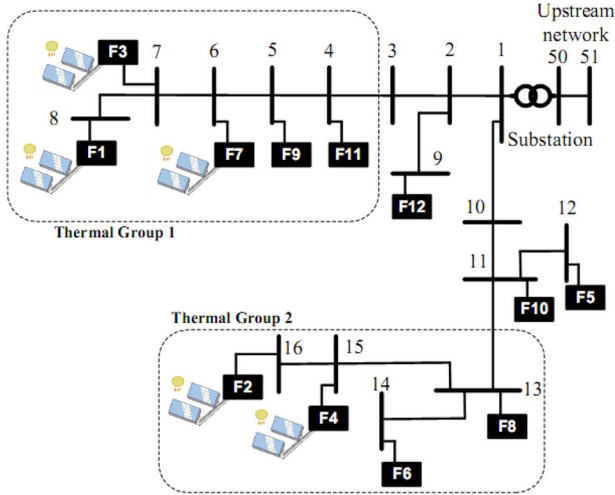


Fig. 2. Single-line diagram of the 18-bus IEEE distribution system [40].

 TABLE I
 INFORMATION OF THE CHP SYSTEMS

Factory	Generator Type*	Pmin [kW]	Pmax [kW]	OMVAR (Eq. 3)	HR (Eq. 4)	α (Eq. 14)
1	GT	500	5000	0.0059	13284	1.84
2	NG	300	3000	0.009	10286	1.2
3	NG	300	3000	0.009	10286	1.2
4	NG	100	1000	0.009	10588	1.36
5	GT	100	1000	0.0096	16438	2.45
6	NG	100	1000	0.0096	16438	2.45
7	NG	30	300	0.013	11613	1.85
8	NG	30	300	0.013	11613	1.85
9	NG	30	300	0.013	11613	1.85
10	NG	10	100	0.018	12000	2.05
11	NG	10	100	0.018	12000	2.05
12	MT	10	100	0.015	13846	1.71

*) GT: gas turbine, NG: natural gas engine, MT: microturbine.

Equation (14) guarantees that the thermal demand of the l th thermal group at hour h will be provided by CHPs and/or boilers. In other words for each thermal group, the thermal power produced by CHPs and the boilers at each hour should be greater than or equal to the required heat [36].

Network Security Constraints:

- Lines capacity
Power flow limits on lines can be formulated as [37]

$$|P_{ij,h}| \leq P_{ij}^{max}. \quad (15)$$

- Bus voltages

$$V_i^{min} \leq V_{i,h} \leq V_i^{max}. \quad (16)$$

Generation Constraints:

- Limit of power generations

$$P_i^{min} \leq P_{i,h}^{CHP} \leq P_i^{max} \quad (17)$$

$$Q_i^{min} \leq Q_{i,h}^{CHP} \leq Q_i^{max}. \quad (18)$$

- Heat output limit for boilers

$$b_{i,h} \leq b_i^{max}. \quad (19)$$

PV Storage Constraints [38]:

The PV generation system at each factory is coupled with PV storage. The following constraints are associated with the PV storages:

- PV storage energy balance

$$E_{i,h}^S = E_{i,h-1}^S + \eta_i^{S, ch} * P_{i,h}^{S, ch} * \Delta h - \frac{1}{\eta_i^{S, Dch}} * P_{i,h}^{S, Dch} * \Delta h. \quad (20)$$

- PV storage charge and discharge rates

$$P_{i,h}^{S, ch} \leq P_i^{S, ch, max} \quad (21)$$

$$P_{i,h}^{S, Dch} \leq P_i^{S, Dch, max}. \quad (22)$$

- PV storage capacity limits

$$E_{i,h}^{S, min} \leq E_{i,h}^S \leq E_i^{S, max}. \quad (23)$$

PEV Dynamic Constraints:

Finally, the following constraints associated with PEVs are also included in the DOPF formulation:

- PEV battery energy balance [27]

$$E_{k,h}^v = E_{k,h-1}^v + \eta_k^v * P_{i,k,h}^{V, ch} * \Delta h. \quad (24)$$

- PEV battery charge rate [27]

$$P_{i,k,h}^{V, ch} \leq P_k^{V, ch, max}. \quad (25)$$

- PEV battery capacity limit [27]

$$E_{k,h}^v \leq E_k^{V, max}. \quad (26)$$

- Preferred PEV plug-out time

$$E_{k,h}^v = E_k^{V, max} \quad \forall k \& \forall h = h_{po,k}. \quad (27)$$

Equation (27) guarantees that PEV batteries will be fully charged before their preferred plug-out times.

The above-mentioned modified DOPF formulation (1)–(7) and constraints (8)–(27) is a nonlinear programming problem that can be solved by most optimization methods. In this paper, the commercial General Algebraic Modeling System software package (GAMS [39]) is used to solve the DOPF problem using branch and bound algorithm.

IV. IMG TEST SYSTEM WITH PEVS AND PV GENERATION SYSTEMS COUPLED WITH PV STORAGES

The test system is an 18-bus, 33-kV [40] IMG consisting of 12 factories with CHP systems, PV generation systems coupled with PV storages and 6 types of PEVs (Fig. 2). The CHP systems data is given in Table I [41]. All factories cooperate in generating electricity. However, only neighboring factories (Fig. 2, groups 1–2) are allowed to participate in acquiring the required heat. The boilers data and CHP parameters are provided in Table II and the Appendix, respectively.

TABLE II
INFORMATION OF THE BOILERS

Factory	Efficiency	Pmax* [kW]
1	0.8	2000
2	0.83	1000
3	0.85	1000
4	0.9	500
6	0.9	500
7	0.85	200
8	0.8	200
9	0.85	200
11	0.83	200

*) Indicates thermal power

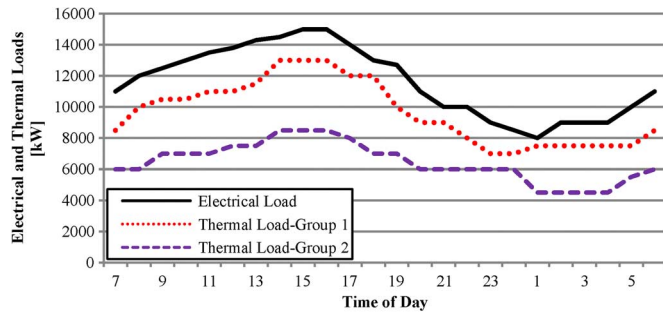


Fig. 3. Forecasted IMG electrical (without PEV charging) and thermal loads.

TABLE III
FACTORY-LOAD DISTRIBUTION FACTORS

Factory	1	2	3	4	5	6
Factory load	0.327	0.197	0.197	0.066	0.066	0.066
Factory	7	8	9	10	11	12
Factory load	0.02	0.02	0.02	0.007	0.007	0.007

The forecasted IMG electric (without any PEV charging) and thermal loads are presented in Fig. 3 while Table III shows load distribution factors of the factories. The simulated PEV types [42]–[44] and details of their ownerships are presented in Table IV and the Appendix, respectively. It is assumed that each PEV has 10% of its total energy when plugged-in and the charging efficiency is 90%. Fig. 4 shows the 24 hours predicted PV generation used in the simulations which is based on the information provided in [45]. The percentages of PV generation and PV storage associated with factories 1, 2, 3, 4 and 7 are 40%, 30%, 10%, 10%, and 10%, respectively. The installed PV storage capacity in the IMG is assumed to be 1000 kWh with charging/discharging efficiency of 90%. The operation and maintenance cost of PV generation system is assumed to be 0.005\$/kWh [34]. The electricity price at the peak hours (10:00 to 19:00) is 0.17\$/kWh, otherwise it is assumed to be 0.09\$/kWh while the gas price at all hours is 0.03\$/kWh [46]. The IMG will sell the electricity to the upstream network at 90% of the purchasing price [$SC = 0.9$ in (7)]. The capacity of the line connecting IMG to the upstream network is equal to 1500 kW. The voltage limits V_i^{min} , and V_i^{max} in (16) are 0.95 pu and 1.05 pu, respectively.

TABLE IV
INFORMATION OF THE SIMULATED PEVS [42]–[44]

PEV Type	PEV Group	Number of PEVs	Battery Size [kWh] (Eq. 26)	Maximum Power Charge [kW] (Eq. 25)	Number of Daily Charging	Plug-in Time/ Preferred Plug-Out Time (Eq. 27)
Light service vehicles	PEV-L1	40	16	2.3	1	(4pm/6am)
	PEV-L2	60	24	4	1	(4pm/6am)
Heavy service vehicles such as personnel buses, delivery trucks, etc.	PEV-H1	10	170	24	1	(6pm/5am)
	PEV-H2	30	85	14	1	(5pm/6am)
Large industrial vehicles requiring fast charging such as picker trucks, lift trucks, etc.	PEV-I1	20	100	100	2	(12pm/2pm), (5pm/6am)
	PEV-I2	12	200	200	3	(11am/1pm), (4pm/6pm), (10pm/6am)

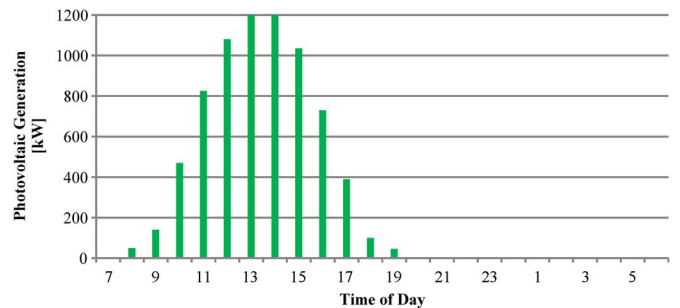


Fig. 4. Predicted PV generation.

V. SIMULATION RESULTS

To show the performances of the proposed formulation, the test system of Fig. 2 is simulated in stand-alone and grid-connected modes without/with considering PEVs and/or PV generation systems. Eleven case studies (Tables V) are simulated and analyzed. The first six cases explore the ability of the proposed approach in scheduling the generation units in conventional IMGs. The remaining cases will show the impacts of PEVs, PV generation systems and PV storages.

A. IMG Generation Scheduling Without PEVs and PV Generation Systems (Cases 1–6, Table V)

- *IMG in Stand-Alone Mode (Cases 1–2, Table V)*: Case 1 considers the situation that each factory independently produces its own demand. Obviously, this will be the most expensive scenario. In Case 2, there is no connection to the upstream network and MGC manages the IMG through cooperation of its own factories. Table VI compares the cost of case studies after the implementation of the proposed method. The overall cost in Case 1 is \$38 422 which is reduced to \$29 859 for the second case.
- *IMG in Grid-Connected Mode (Cases 3–6, Table V)*: Four case studies (Cases 3–6, Table V) are considered to investigate the performance of the proposed method in grid-connected mode with the possibility of exchanging electricity

TABLE V
SIMULATED CASE STUDIES

Case Study	PEV Coordination	PV Generation	Operation Strategy*
IMG in Stand-Alone Mode			
1	-	-	Independent
2	-	-	Cooperative
IMG in Grid-Connected Mode (buying electricity)			
3	-	-	Independent
4	-	-	Cooperative
IMG in Grid-Connected Mode (buying & selling electricity)			
5	-	-	Independent
6	-	-	Cooperative
7	Uncoordinated	-	Cooperative
8	Coordinated, fixed charge rate	-	Cooperative
9	Coordinated, variable charge rate	-	Cooperative
10	Coordinated, fixed charge rate	✓	Cooperative
11	Coordinated, variable charge rate	✓	Cooperative

*) Independent: Each factory manages its own systems, Cooperative: MGC manages the IMG operation with the proposed method.

TABLE VI
COMPARISON OF COSTS AND SAVINGS ASSOCIATED WITH THE CASE STUDIES

Case	Cost (Eqs. 1 & 2) [\$]	Revenue (Eqs. 1 & 7) [\$]	Overall Cost (Eq. 1) [\$]	Thermal Saving [MWh]	Cost of PEVs Charging [\$]
1	38422	-	38422	352.6	-
2	29859	-	29859	378.0	-
3	31565	-	31656	353.7	-
4	29751	-	29751	382.3	-
5	32495	1401	31094	356.2	-
6	30971	1385	29586	385.3	-
7	32667	610	32057	385.3	2471
8	32452	673	31778	385.3	2192
9	32119	594	31525	385.3	1939
10	31863	1601	30262	385.3	676
11	31581	1833	29748	385.3	162

with the upstream network. In all cases, the IMG can purchase electricity from the upstream network while in Cases 5–6 it can also sell the electricity.

Table VII shows the cooperation schedule of the generators in Case 6 after performing the optimization. Generators 10, 11, and 12 are merely turned on during the peak interval so that the IMG can sell more power to the upstream market. It can also be observed that mostly during the peak hours, all generators are running at their highest production levels in order to sell more electricity to the network and gain more profit. This will naturally minimize the overall IMG cost. For example at 15:00 (Table VII), all generators are generating maximum electric power and the total cost of electricity production is \$1677.136. In other words, the IMG electricity production cost at this hour is \$0.11/kWh, while the produced electricity surplus is sold at $0.9 \times (0.17\$/\text{kWh}) = \$0.153/\text{kWh}$. This revenue can reduce the cost of supplying heat and electricity in the IMG. Tables VIII and IX show the amount of purchased and sold

electricity from/to the upstream network at different hours. According to these tables, the IMG prefers to only purchase electricity from the upstream network when the price is low. Otherwise, it will sell its excess electricity to increase the profit.

Simulation results also indicate that all boilers of Group 1 are turned off as the required thermal power of this group has been supplied by the CHP systems. However, the situation is different with Group 2 as boilers 4 and 6 are also contributing to fully satisfy the thermal power requirement. Table X presents the production planning of the boilers of Group 2. According to the results, the IMG (with thermal energy consumption of 387 MWh in 24 hours) can save 385 MWh of the required heat by using the CHPs and acquire only about 2 MWh of the required thermal from its boilers.

The total cost of IMG in Case 6 (including electricity production, heat production and selling the electricity) is \$30 971 while the revenue of selling electricity to the upstream network is \$1385. Therefore, the overall cost is $\$30\,971 - \$1385 = \$29\,586$. The important point is that by implementing the proposed optimization with the aim of increasing the profit, the solution will be generated in a way that most of IMG potentials are utilized. In other words, MGC will sell electricity to the upstream network if the cost of generating electricity is cheaper than the purchased price.

In Case 5, each factory can individually buy/sell electricity from/to the upstream network (by using 1/12 capacity of the line connecting IMG to the upstream network) and independently manage its own systems. In this case and also in Case 3 there is no guaranty to keep the voltage profiles in acceptable bounds. Note that if the IMG is only permitted to purchase from the upstream network (Cases 3 and 4), the final cost of supplying the loads will be \$31 656 and \$29 751, respectively.

B. IMG Generation Scheduling With Uncoordinated and Coordinated PEV Charging Without PV Generation (Cases 7–9, Table V)

The rating and charging characteristics of PEVs in IMG applications such as picker and lift trucks are different than those employed in the residential networks as they usually have large batteries and may require fast charging during peak load hours. Therefore, their uncoordinated fast charging activities can significantly affect the operation of IMGs.

The worst scenario may occur when many PEVs are charged with a fixed charge rate as soon as arriving at their stations (Case 7). Fig. 5 shows the daily load profile of IMG for Cases 1–9. In Case 7, uncoordinated PEV charging has increased the loading level from 15 000 kW (without PEVs) to approximately 18 000 kW (with PEVs) at 16:00. As shown in Fig. 6, this situation results in overloading of the connecting line between IMG and network at some hours between 16:00–17:00. Also this uncoordinated charging strategy may affect the voltage profile (Fig. 7, hour 16:00).

By coordinating PEV charging activities (Cases 8–9), the proposed method can manage the IMG operation such that the overall operation cost is reduced while all system constraints are satisfied. In fact, MGC uses the proposed DOPF to schedule PEV charging overnight and consequently perform peak load shaving (Case 8). Furthermore, if MGC chooses the variable charging strategy, the load profile becomes more flat.

TABLE VII
COOPERATION SCHEDULE (IN kW) OF GENERATORS IN THE FACTORIES (CASE 6)

Hour	Factory (Generator) Number											
	1	2	3	4	5	6	7	8	9	10	11	12
7	2663	2814	3000	1000	274	289	0	300	0	0	0	0
8	3343	3000	3000	1000	367	198	105	300	30	0	0	0
9	3536	3000	3000	1000	309	606	183	300	30	0	0	0
10	5000	3000	3000	1000	821	606	300	300	300	100	100	100
11	5000	3000	3000	1000	1000	776	300	300	300	100	100	100
12	5000	3000	3000	1000	1000	868	300	300	300	100	100	100
13	5000	3000	3000	1000	1000	1000	300	300	300	100	100	100
14	5000	3000	3000	1000	1000	1000	300	300	300	100	100	100
15	5000	3000	3000	1000	1000	1000	300	300	300	100	100	100
16	5000	3000	3000	1000	1000	1000	300	300	300	100	100	100
17	5000	3000	3000	1000	1000	1000	300	300	300	100	100	100
18	5000	3000	3000	1000	821	606	300	300	300	100	100	100
19	3478	3000	3000	1000	323	606	0	300	0	0	0	0
20	2935	2814	3000	1000	275	289	0	300	0	0	0	0
21	2491	2325	3000	1000	138	528	141	300	300	0	0	0
22	2391	2465	3000	1000	163	460	0	300	0	0	0	0
23	1848	2332	3000	1000	100	525	0	300	0	0	0	0
24	1848	1812	3000	1000	0	772	0	300	0	0	0	0
1	1735	1950	3000	1000	100	100	83	300	300	0	0	0
2	2120	2154	3000	1000	181	0	0	300	0	0	0	0
3	2120	2154	3000	1000	181	0	0	300	0	0	0	0
4	2120	2154	3000	1000	181	0	0	300	0	0	0	0
5	2120	2545	3000	1000	213	217	0	300	0	0	0	0
6	2663	2814	3000	1000	274	289	0	300	0	0	0	0

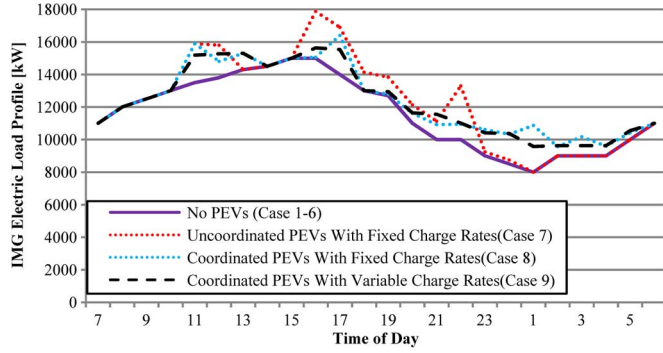


Fig. 5. The 24-hour electrical load profile for Cases 1-9.

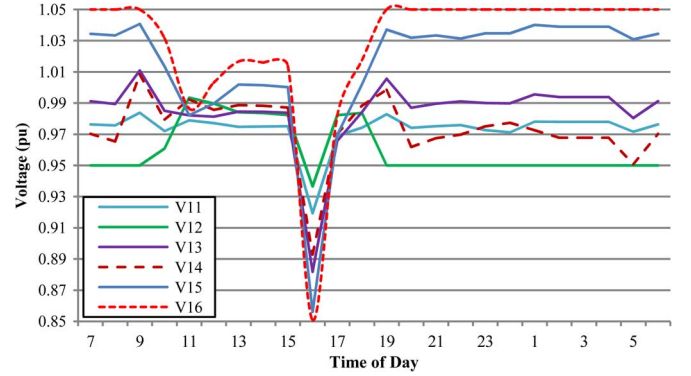


Fig. 7. Voltage profile in Case 7.

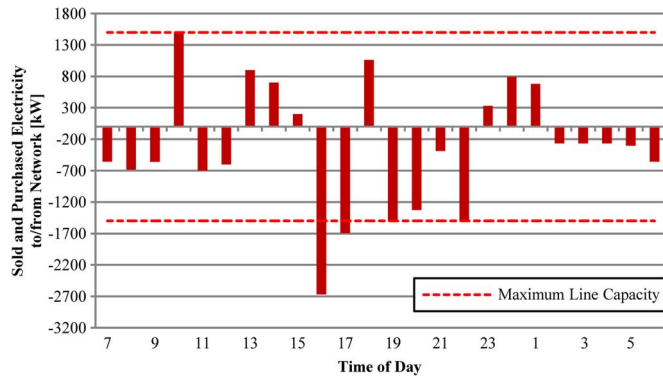


Fig. 6. Purchased and sold electricity from/to the upstream network, Case 7. Positive and negative values indicate the sold and purchased electricity, respectively.

TABLE VIII
PURCHASED ELECTRICITY FROM THE UPSTREAM NETWORK (CASE 6)

Hour	2	3	4	5	6	7
Purchased Electricity [kW]	367	367	367	802	825	825
Hour	8	9	19	20	22	23
Purchased Electricity [kW]	773	631	1114	509	360	110

TABLE IX
SOLD ELECTRICITY TO THE UPSTREAM NETWORK (CASE 6)

Hour	1	10	11	12	13	14
Sold Electricity [kW]	436	1500	1396	1213	874	684
Hour	15	16	17	18	21	24
Sold Electricity [kW]	198	198	1154	1500	116	90

Fig. 9 compares the overall schedule and power requirements for coordinated PEVs with fixed and variable charge rates. Clearly, the proposed DOPF nicely utilizes the variable

charge strategy to distribute the required power for charging PEVs and shift them to off peak hours as much as possible.

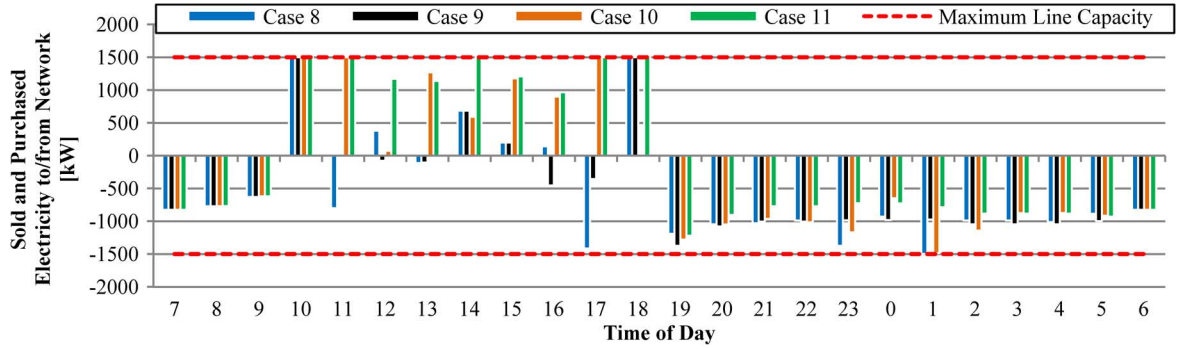


Fig. 8. Purchased and sold electricity from/to the upstream network, Case 8–11. Positive and negative values indicate the sold and purchased electricity, respectively.

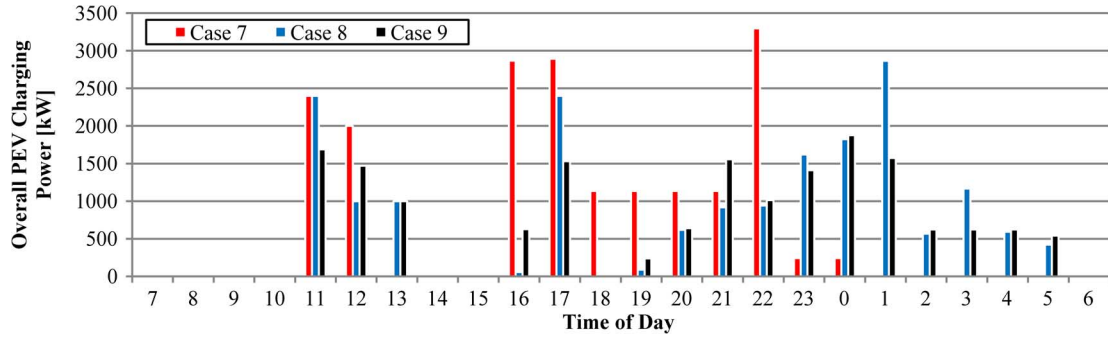


Fig. 9. Coordinated charging schedule of PEVs over 24 hours.

TABLE X
PRODUCTION OF THE BOILERS IN GROUP 2 (CASE 6)

Hour	14	15	16	17	24
Boiler of Factory 4 [kW]	267	267	267	20	9
Boiler of Factory 6 [kW]	267	267	267	20	9

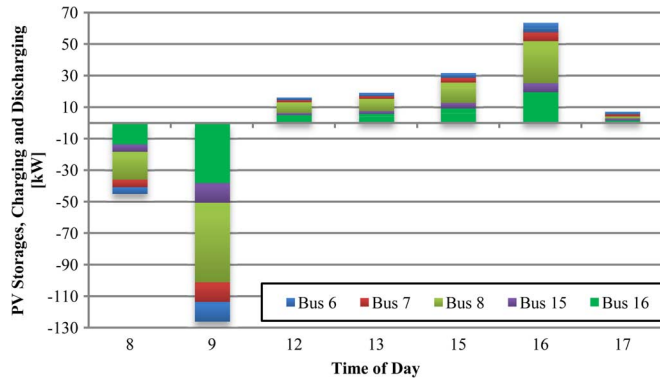


Fig. 10. Charge/discharge schedule of PV storages (Case 11). Negative and positive values indicate the charge and discharge power, respectively.

From Table VI, it can be seen that the overall cost of PEV operation is considerably reduced from \$2471 (uncoordinated) to \$2192 and \$1939 for coordinated charging with fixed and variable charge rates, respectively.

C. IMG Generation Scheduling With PEVs and PV Generation Systems (Cases 10–11, Table V)

Application of PV generation systems in IMGs is investigated in Case studies 10–11. The proposed method will utilize

PV generation systems coupled with PV storages to optimize the schedule of selling and buying electricity at the peak hours (11:00–17:00) in order to minimize the overall cost of IMG (Fig. 8). This is done by charging PV storage elements during some hours and selling the stored energy at appropriate times to increase the profit. Fig. 10 shows the charge and discharge schedule of PV storages for Case 11. According to the simulation results of this paper, employment of PV generation systems coupled with PV storages and coordination of PEVs with variable charging rates will result in considerable decrease in vehicles battery charging costs (Table VI, last column) and will also reduce the overall cost of IMG (Table VI, column 4).

D. Handling Overloading and Low Voltage Situation

As demonstrated in Figs. 8 and 9, MGC can utilize the proposed generation scheduling method to handle overloading and low voltage situations (Figs. 6 and 7) by considering three strategies: 1) PEV charging with fixed charge rates (Case 8), 2) PEV charging with variable charge rates (Case 9), or 3) PEV charging with fixed/variable charge rates and PV generation systems coupled with PV storages (Cases 10–11).

VI. CONCLUSION

A new generation scheduling method coordinated with PEVs charging based on DOPF is proposed and demonstrated for an IMG consist of 12 factories with CHP systems, PV generation systems coupled with PV storages and 6 types of PEVs. The main capabilities of the proposed coordination approach are as follows:

TABLE XI
ASSUMED OWNERSHIPS OF THE SIMULATED PEVS (TABLE IV)

Factory	PEV Type					
	L1	L2	H1	H2	I1	I2
1	5	10	5	8	6	5
2	4	10	4	5	4	4
3	4	4	1	4	3	2
4	3	4	-	5	3	1
5	3	4	-	4	-	-
6	3	4	-	4	1	-
7	3	4	-	-	3	-
8	3	4	-	-	-	-
9	3	4	-	-	-	-
10	3	4	-	-	-	-
11	3	4	-	-	-	-
12	3	4	-	-	-	-

- Both network security and factories constraints (including PEVs and PV storages dynamic constraints) are included in DOPF formulation.
- It minimizes the overall cost of IMG by optimizing the hourly heat and electricity generation schedules for individual factories.
- The optimization problem is subjected to both electric and thermal requirements considering the possibilities of heat transfer between adjacent factories.
- It manages the factories such that part of required electricity is purchased from the upstream network when the price of electricity is lower than the generation cost. Otherwise, the IMG will sell electricity to increase the overall profit.
- It considers PEVs with time and energy related constraints as coordinated loads and optimizes their charging rates in order to minimize the cost associated with vehicle charging and to maintain the voltage profile within the acceptable limits (Table VI, Cases 8–11).

Finally, based on the analyses of this paper, introduction of PV generation systems coupled with PV storages in IMGs could have positive effects on their scheduling solution and minimizing the overall cost (Table VI, Cases 10–11) since the peak of most industrial electricity loads occur during daytime and usually coincide with the maximum output of PV generation.

APPENDIX OWNERSHIPS OF PEVS AND CHP PARAMETERS

The assumed ownerships of the simulated PEVs (Table IV) are presented in Table XI.

The thermodynamic parameters of CHP systems used in the simulations are [32] as follows:

- Heat Rate [HR, (4) and Table I]—HR in kilo joule per kilowatt hour (kJ/kWh) indicates how much fuel is required to produce a unit of electric energy. The electric efficiency of a generation device can be determined by converting HR to kJ/kJ (dividing by 3600 kJ/kWh) and taking the inverse.
- Waste Heat Factor [α , (14) and Table I]— α is a dimensionless ratio of energy terms that describes how much useful heat energy is generated per electric energy produced by a given generation technology.

REFERENCES

- [1] S. Chowdhury, S. P. Chowdhury, and P. Crossley, *Microgrids and Active Distribution Networks*. London, U.K.: IET, 2009, pp. 15–16.
- [2] U. S. Department of Energy, Combined Heat and Power—A Decade of Progress, Aug. 2009. [Online]. Available: http://www.pacificcleanenergy.org/DOE_CHPreport.pdf.
- [3] F. Starfelt and J. Yan, “Case study of energy systems with gas turbine cogeneration technology for an eco-industrial park,” *Int. J. Energy Res.*, vol. 32, no. 12, pp. 1128–1135, 2008.
- [4] Capstone Team, “Capstone microturbines,” 2010. [Online]. Available: http://www.capstoneturbine.com/_docs/Product%20Catalog_ENGLISH_LR.pdf.
- [5] F. E. Pierce, Summary of results from testing a 30 kW microturbine and combined heat and power (CHP) system, Federal Energy Management Program—U.S. Department of Energy, DOE/EE-0316, May 2007.
- [6] N. Wägar, “Wind-diesel or wind-gas, cases and possibilities by Wärsilä,” in *Proc. Int. Wind-Diesel Workshop*, 2008. [Online]. Available: http://apps1.eere.energy.gov/tribalenergy/pdfs/wind_akco10.pdf.
- [7] R. J. Yinger, Behavior of capstone and honey well microturbine generators during load changes, Ernest Orlando Lawrence Berkeley National Lab., LBNL-49095, Feb. 2004. [Online]. Available: certs.lbl.gov/pdf/49095.pdf.
- [8] J. Herbretreau, V. Courtecuisse, L. Peng, P. Degobert, B. Robyns, and B. Francois, “Association of PV, gas micro turbine and short term storage system to participate in frequency control,” in *Proc. Int. Conf. Renewable Energies and Power Quality*, Santander, Spain, 2008, pp. 1–6.
- [9] T. Niknam, M. R. Narimani, J. Aghaei, and R. Azizipanah-Abarghooee, “Improved particle swarm optimisation for multi-objective optimal power flow considering the cost, loss, emission and voltage stability index,” *IET Gen., Transm. Distrib.*, vol. 6, no. 6, pp. 515–527, 2012.
- [10] N. Amjadi, H. Fatemi, and H. Zareipour, “Solution of optimal power flow subject to security constraints by a new improved bacterial foraging method,” *IEEE Trans. Power Syst.*, vol. 27, no. 3, pp. 1311–1323, Aug. 2012.
- [11] C. Y. Chung, W. Yan, and F. Liu, “Decomposed predictor-corrector interior point method for dynamic optimal power flow,” *IEEE Trans. Power Syst.*, vol. 26, no. 3, pp. 1030–1039, Aug. 2011.
- [12] T. Logenthiran, D. Srinivasan, A. M. Khambadkone, and H. N. Aung, “Multiagent system for real-time operation of a microgrid in real-time digital simulator,” *IEEE Trans. Smart Grid*, vol. 3, no. 2, pp. 925–933, Jun. 2012.
- [13] A. K. Basu, A. Bhattacharya, S. Chowdhury, and S. P. Chowdhury, “Planned scheduling for economic power sharing in a CHP-based micro-grid,” *IEEE Trans. Power Syst.*, vol. 27, no. 1, pp. 30–38, Feb. 2012.
- [14] A. G. Tsikalakis and N. D. Hatziargyriou, “Centralized control for optimizing microgrids operation,” *IEEE Trans. Energy Convers.*, vol. 23, no. 1, pp. 241–248, Mar. 2008.
- [15] P. Wan and M. D. Lemmon, “Optimal power flow in microgrids using event-triggered optimization,” in *Proc. American Control Conf.*, Baltimore, MD, USA, 2010, pp. 2521–2526.
- [16] E. Sortomme and M. A. El-Sharkawi, “Optimal power flow for a system of microgrids with controllable loads and battery storage,” in *Proc. Power Systems Conf. Expo.*, 2009, pp. 1–5.
- [17] S. Conti, R. Nicolosi, S. A. Rizzo, and H. H. Zeineldin, “Optimal dispatching of distributed generators and storage systems for MV islanded microgrids,” *IEEE Trans. Power Del.*, vol. 27, no. 3, pp. 1243–1251, Jul. 2012.
- [18] M. A. López, S. Martín, J. A. Aguado, and S. de la Torre, “Optimal microgrid operation with electric vehicles,” in *Proc. Innovative Smart Grid Technologies Conf.*, 2011, pp. 1–8.
- [19] P. Asmus, A. Cornelius, and C. Wheelock, Microgrid—Islanded Power Grids and Distributed Generation for Community, Commercial, Institutional Applications, 2009, Pike Research Report, 4Q.
- [20] H. S. V. S. K. Nunna and S. Ashok, “Optimal management of microgrids,” in *Proc. Innovative Technologies for an Efficient and Reliable Electricity Supply Conf.*, Waltham, MA, USA, 2010, pp. 448–453.
- [21] W. Su, H. Rahimi-Eichi, W. Zeng, and M. Chow, “A survey on the electrification of transportation in a smart grid environment,” *IEEE Trans. Ind. Appl.*, vol. 8, no. 1, pp. 1–10, 2012.
- [22] M. E. Khodayar, L. Wu, and M. Shahidepour, “Hourly coordination of electric vehicle operation and volatile wind power generation in SCUC,” *IEEE Trans. Smart Grid*, to be published.

- [23] C. Liu, J. Wang, A. Botterud, Y. Zhou, and A. Vyas, "Assessment of impacts of PHEV charging patterns on wind-thermal scheduling by stochastic unit commitment," *IEEE Trans. Smart Grid*, vol. 3, no. 2, pp. 675–683, Jun. 2012.
- [24] A. Y. Saber and G. K. Venayagamoorthy, "Intelligent unit commitment with vehicle-to-grid—A cost-emission optimization," *J. Power Sources*, vol. 195, no. 3, pp. 898–911, 2010.
- [25] S. Deilami, A. S. Masoum, P. S. Moses, and M. A. S. Masoum, "Real-time coordination of plug-in electric vehicle charging in smart grids to minimize power losses and improve voltage profile," *IEEE Trans. Smart Grid*, vol. 2, no. 3, pp. 456–467, 2011.
- [26] O. Sundström and C. Binding, "Flexible charging optimization for electric vehicles considering distribution grid constraints," *IEEE Trans. Smart Grid*, vol. 3, no. 1, pp. 26–37, Mar. 2012.
- [27] T. Sousa, H. Morais, Z. Vale, P. Faria, and J. Soares, "Intelligent energy resource management considering vehicle-to-grid: A simulated annealing approach," *IEEE Trans. Smart Grid*, vol. 3, no. 1, pp. 535–542, Mar. 2012.
- [28] EPIA Team, Solar Europe Industry Initiative Implementation plan 2010–2012. May 2010. [Online]. Available: http://ec.europa.eu/energy/technology/initiatives/doc/pv_implementation_plan_final.pdf.
- [29] U. S. Department of Energy, One Million Electric Vehicles by 2015, Feb. 2011. [Online]. Available: http://www1.eere.energy.gov/vehicle-sandfuels/pdfs/1_million_electric_vehicles_rpt.pdf.
- [30] H. Beltran, E. Pérez, N. Aparicio, and P. Rodríguez, "Daily solar energy estimation for minimizing energy storage requirements in PV power plants," *IEEE Trans. Sustain. Energy*, vol. 4, no. 2, pp. 474–481, Apr. 2013.
- [31] M. K. C. Marwali, M. Haili, S. M. Shahidehpour, and K. H. Abdul-Rahman, "Short term generation scheduling in photovoltaic-utility grid with battery storage," *IEEE Trans. Power Syst.*, vol. 13, no. 3, pp. 1057–1062, Aug. 1998.
- [32] A. S. Siddiqui, R. Firestone, S. Ghosh, M. Stadler, J. L. Edwards, and C. Marnay, Ernest Orlando Lawrence Berkeley National Lab., Distributed Energy Resources With Combined Heat and Power Applications, LBNL-52718, Jun. 2003. [Online]. Available: http://eetd.lbl.gov/ea/EMS/EMS_pubs.html.
- [33] K. M. Maribu and S. Fleten, "Combined heat and power in commercial buildings: Investment and risk analysis," *Energy J.*, vol. 29, no. 2, pp. 1–25, 2008.
- [34] R. Chedid, S. Karaki, and A. Rifai, "Multi-objective design methodology for hybrid renewable energy systems," in *Proc. Power Tech Conf.*, St. Petersburg, Russia, 2005, pp. 1–6.
- [35] R. Priddle, Distributed Generation in Liberalised Electricity Markets, International Energy Agency, 2002, pp. 25–26.
- [36] Y. Zokaa, A. Sugimoto, N. Yorino, K. Kawahara, and J. Kubokawa, "An economic evaluation for an autonomous independent network of distributed energy resources," *Elect. Power Syst. Res.*, vol. 77, pp. 831–838, 2007.
- [37] T. Niknam, M. R. Narimani, J. Aghaei, S. Tabatabaei, and M. Nayeripour, "Modified honey bee mating optimisation to solve dynamic optimal power flow considering generator constraints," *IET Gen., Transm., Distrib.*, vol. 5, no. 10, pp. 989–1002, 2011.
- [38] M. Stadler, C. Marnay, A. Siddiqui, J. Lai, B. Coffey, and H. Aki, "Effect of Heat and Electricity Storage and Reliability on Microgrid Viability: A Study of Commercial Buildings in California and New York States," Ernest Orlando Lawrence Berkeley National Lab., LBNL-1334E, Mar. 2009. [Online]. Available: <http://der.lbl.gov/sites/der.lbl.gov/files/lbnl-1334e.pdf>.
- [39] General Algebraic Modeling System (GAMS), 2010. [Online]. Available: <http://www.gams.com>.
- [40] M. A. S. Masoum, A. Jafarian, M. Ladjevardi, E. F. Fuchs, and W. M. Grady, "Fuzzy approach for optimal placement and sizing of capacitor banks in the presence of harmonics," *IEEE Trans. Power Del.*, vol. 19, no. 2, pp. 822–829, Apr. 2004.
- [41] R. Firestone, DER-CAM natural gas technology data, Lawrence Berkeley National Lab., Jan. 2004. [Online]. Available: <http://der.lbl.gov/der-cam/technology-data-archive>.
- [42] Power Vehicle Innovation Team, Electric Cowl-Chassis 7, 2T GVW Daily, Oct. 2011, 2nd ed. [Online]. Available: <http://www.pvi.fr>.
- [43] VIA Motors Team, Extended-Range Electric Fleet Vans From VIA Motors. [Online]. Available: <http://www.viamotors.com/>.
- [44] J. D. Graham, Plug-In Electric Vehicles: A Practical Plan for Progress, School of Public and Environmental Affairs, Indiana Univ., Feb. 2011.
- [45] H. Kanchev, D. Lu, F. Colas, V. Lazarov, and B. Francois, "Energy management and operational planning of a microgrid with a PV-based active generator for smart grid applications," *IEEE Trans. Ind. Electron.*, vol. 58, no. 10, pp. 4583–4592, Oct. 2011.
- [46] C. Marnay, G. Venkataramanan, M. Stadler, A. S. Siddiqui, R. Firestone, and B. Chandran, "Optimal technology selection and operation of commercial-building microgrids," *IEEE Trans. Power Syst.*, vol. 23, no. 3, pp. 975–982, Aug. 2008.

S. Y. Derakhshandeh (S'12) received the B.Sc. and M.Sc. degrees in electrical engineering from Power and Water University of Technology, Tehran, Iran, in 2003 and Isfahan University of Technology, Isfahan, Iran, in 2006, respectively. Currently he is pursuing the Ph.D. degree at Isfahan University of Technology.

He is a visiting scholar at Curtin University, Perth, Australia, from April 20 to October 20, 2012. His main interests are power system analysis, electricity market, and microgrid.

Amir S. Masoum (S'09–M'11) received the B.S. and M.S. degrees in electrical engineering and electrical utility engineering from the University of Western Australia, WA, Australia, and Curtin University, Perth, WA, Australia, in 2009 and 2010, respectively. He is currently pursuing the Ph.D. degree in electrical engineering at Curtin University, Australia.

Sara Deilami (S'09) received the B.S. degree in electrical engineering from Islamic Azad University, Tehran, Iran, in 2000 and the M.S. degree in electrical engineering from Curtin University, Perth, WA, Australia, in 2011. She is currently pursuing the Ph.D. degree in electrical engineering at Curtin University. She was awarded a Curtin University Postgraduate Scholarship (CUPS) and an Australian Postgraduate Award (APA) scholarship in 2010 and 2011, respectively.

Mohammad A. S. Masoum (S'88–M'91–SM'05) received the B.S., M.S., and Ph.D. degrees in electrical and computer engineering from the University of Colorado, Boulder, CO, USA, in 1983, 1985, and 1991, respectively.

He is the co-author of *Power Quality in Power Systems and Electrical Machines* (New York, NY, USA: Elsevier, 2008) and *Power Conversion of Renewable Energy Systems* (New York, NY, USA: Springer, 2011). Currently, he is a Professor and Discipline Leader for Electrical Power Engineering at the Electrical and Computer Engineering Department, Curtin University, Perth, WA, Australia.

M. E. Hamedani Golshan received the Ph.D. degree in electrical engineering from Isfahan University of Technology, Isfahan, Iran, in 1995.

Currently, he is a Professor at the Electrical and Computer Engineering Department, Isfahan University of Technology. His main interests are power system analysis, power system dynamics, and distributed generation.